High frequency attenuation of S-waves in alluvial deposits of the central Po Plain (northern Italy) - Supplementary data

Gianlorenzo Franceschina [1] and Alberto Tento [2]

[1] *Istituto Nazionale di Geofisica e Vulcanologia, Sezione di Milano, Via Alfonso Corti 12, 20133 Milano, Italy. E-mail: gianlorenzo.franceschina@ingv.it*

[2] *Retired, CNR - Istituto per la Dinamica dei Processi Ambientali, Milano, Italy.*

CONTENTS

1 EXAMPLES OF K-RECORD ESTIMATION

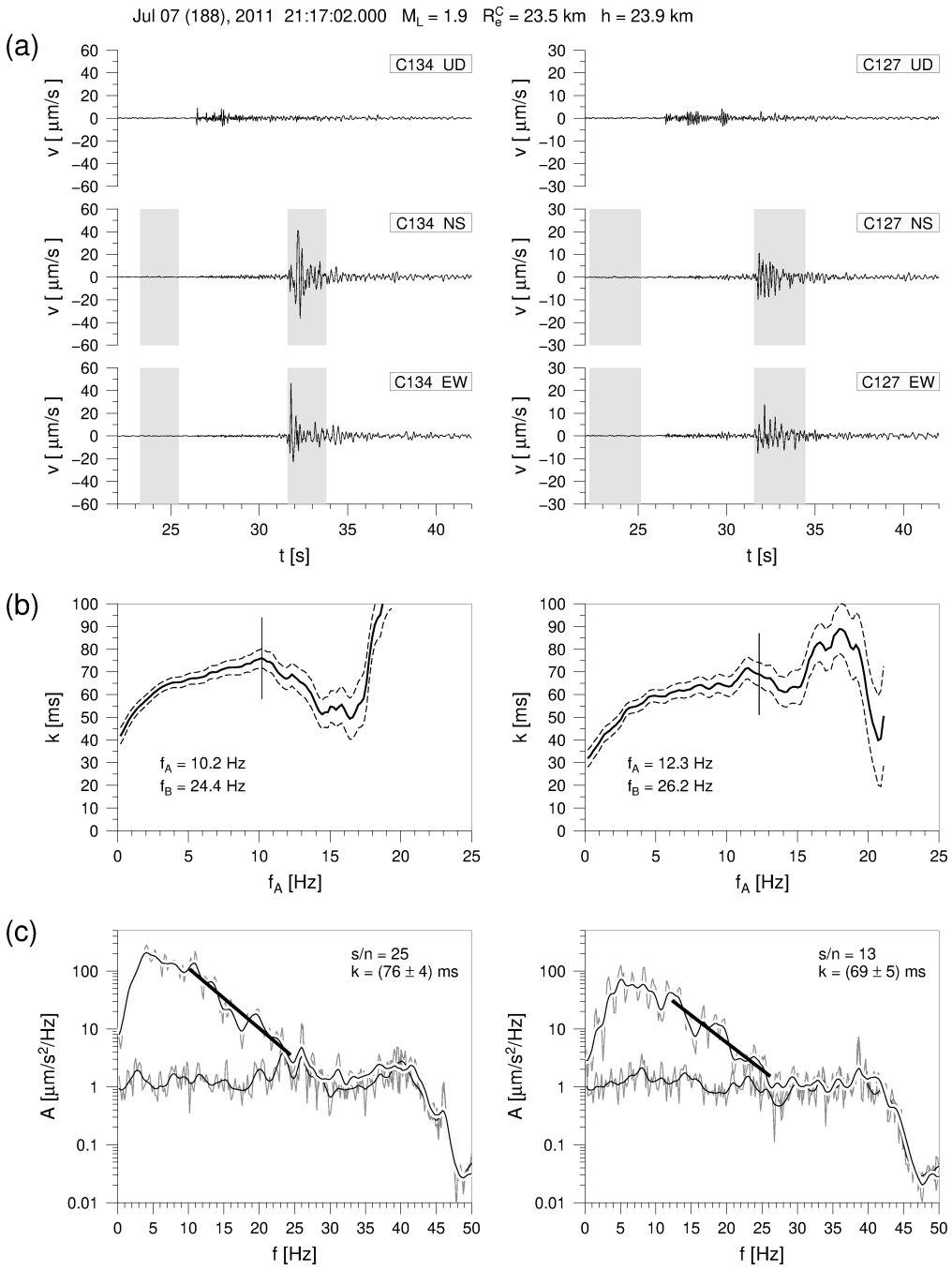

Figure S1. Example of k-record estimation: 7 July 2011 M_L=1.9 earthquake, recorded by stations C134 (surface) and C127 (borehole). R_e^C is the epicentral distance measured from the center of the network. h is depth. (a): velocity records (vertical, NS and EW components) and time windows employed for noise and signal analysis (grey areas). (b): k-record estimates and standard deviations as a function of the lower limit of the frequency band adopted for the linear regression, f_A (solid and dashed lines, respectively). The adopted values of f_A and f_B are also indicated, and the vertical segment marks the chosen value of f_A. (c): signal and noise maximized acceleration spectra and linear regressions used to obtain the k-record estimate. Grey lines: original spectra of signal and noise; black thin line: smoothed noise spectrum; highlighted black thin line: smoothed signal spectrum; black thick line: linear regression. Signal-to-noise ratios, s/n, and k-record estimates are also indicated.

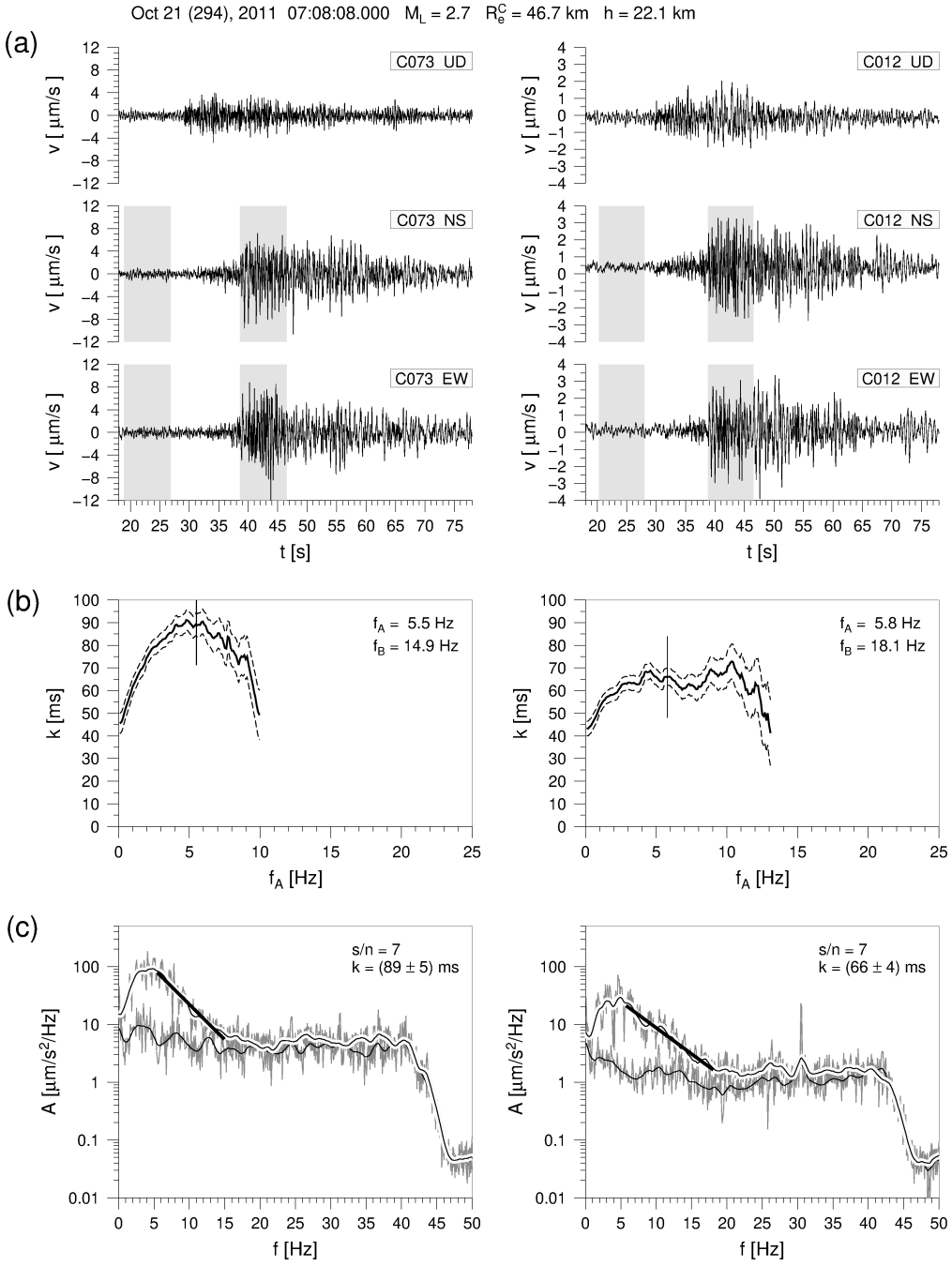

Figure S2. Example of k-record estimation: 21 October 2011 M_L=2.7 event, recorded by stations C073 (surface) and C012 (borehole). R_e^C is the epicentral distance measured from the center of the network. h is depth. (a): velocity records (vertical, NS and EW components) and time windows employed for noise and signal analysis (grey areas). (b): k-record estimates and standard deviations as a function of the lower limit of the frequency band adopted for the linear regression, f_A (solid and dashed lines, respectively). The adopted values of f_A and f_B are also indicated, and the vertical segment marks the chosen value of f_A. (c): signal and noise maximized acceleration spectra and linear regressions used to obtain the k-record estimate. Grey lines: original spectra of signal and noise; black thin line: smoothed noise spectrum; highlighted black thin line: smoothed signal spectrum; black thick line: linear regression. Signal-to-noise ratios, s/n, and k-record estimates are also indicated.

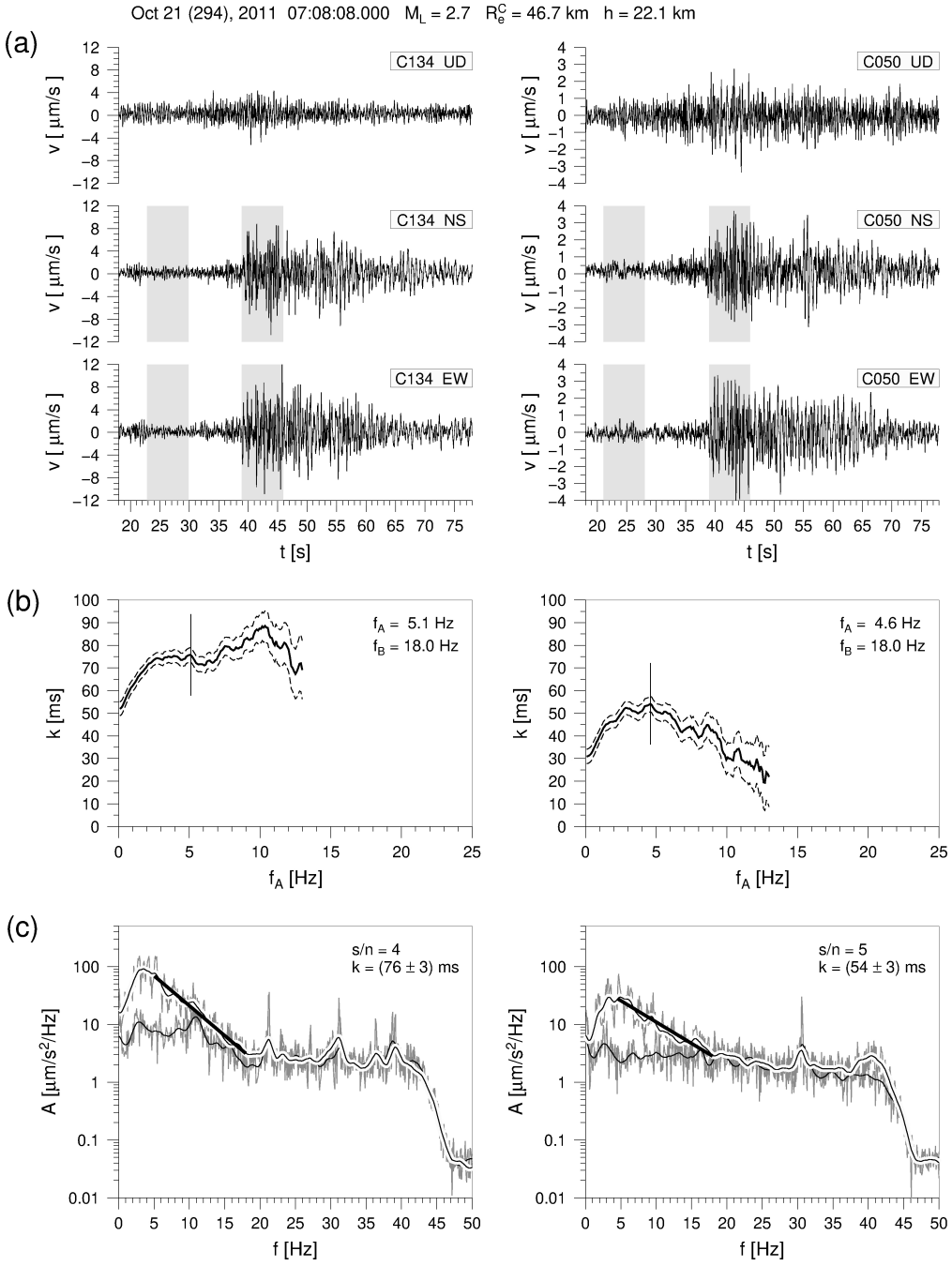

Figure S3. Example of k-record estimation: 21 October 2011 M_L=2.7 event, recorded by stations C134 (surface) and C050 (borehole). R_e^C is the epicentral distance measured from the center of the network. h is depth. (a): velocity records (vertical, NS and EW components) and time windows employed for noise and signal analysis (grey areas). (b): k-record estimates and standard deviations as a function of the lower limit of the frequency band adopted for the linear regression, f_A (solid and dashed lines, respectively). The adopted values of f_A and f_B are also indicated, and the vertical segment marks the chosen value of f_A. (c): signal and noise maximized acceleration spectra and linear regressions used to obtain the k-record estimate. Grey lines: original spectra of signal and noise; black thin line: smoothed noise spectrum; highlighted black thin line: smoothed signal spectrum; black thick line: linear regression. Signal-to-noise ratios, s/n, and k-record estimates are also indicated.

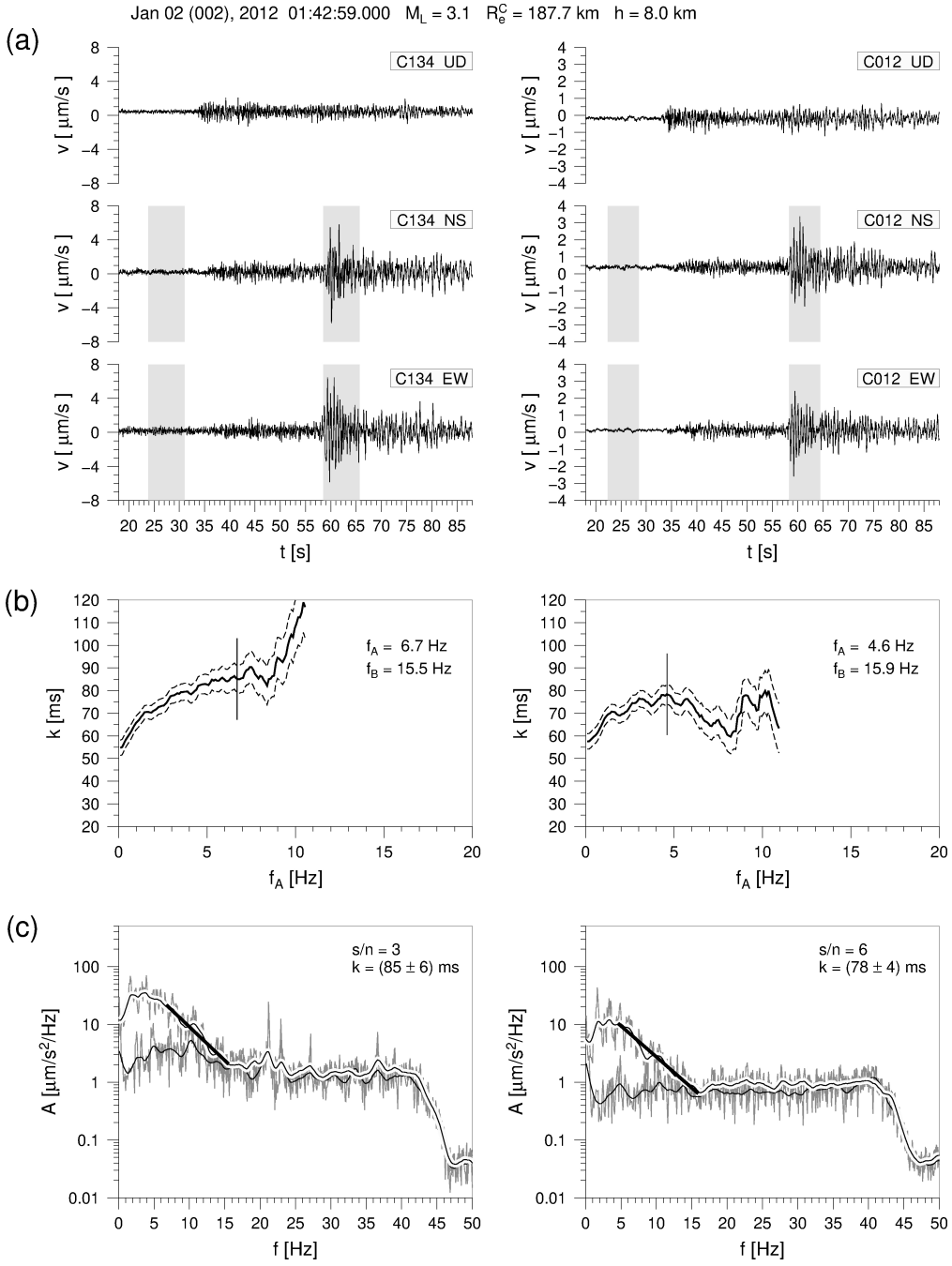

Figure S4. Example of k-record estimation: 2 January 2012 M_L=3.1 event, recorded by stations C134 (surface) and C012 (borehole). R_e^C is the epicentral distance measured from the center of the network. h is depth. (a): velocity records (vertical, NS and EW components) and time windows employed for noise and signal analysis (grey areas). (b): k-record estimates and standard deviations as a function of the lower limit of the frequency band adopted for the linear regression, f_A (solid and dashed lines, respectively). The adopted values of f_A and f_B are also indicated, and the vertical segment marks the chosen value of f_A. (c): signal and noise maximized acceleration spectra and linear regressions used to obtain the k-record estimate. Grey lines: original spectra of signal and noise; black thin line: smoothed noise spectrum; highlighted black thin line: smoothed signal spectrum; black thick line: linear regression. Signal-to-noise ratios, s/n, and k-record estimates are also indicated.

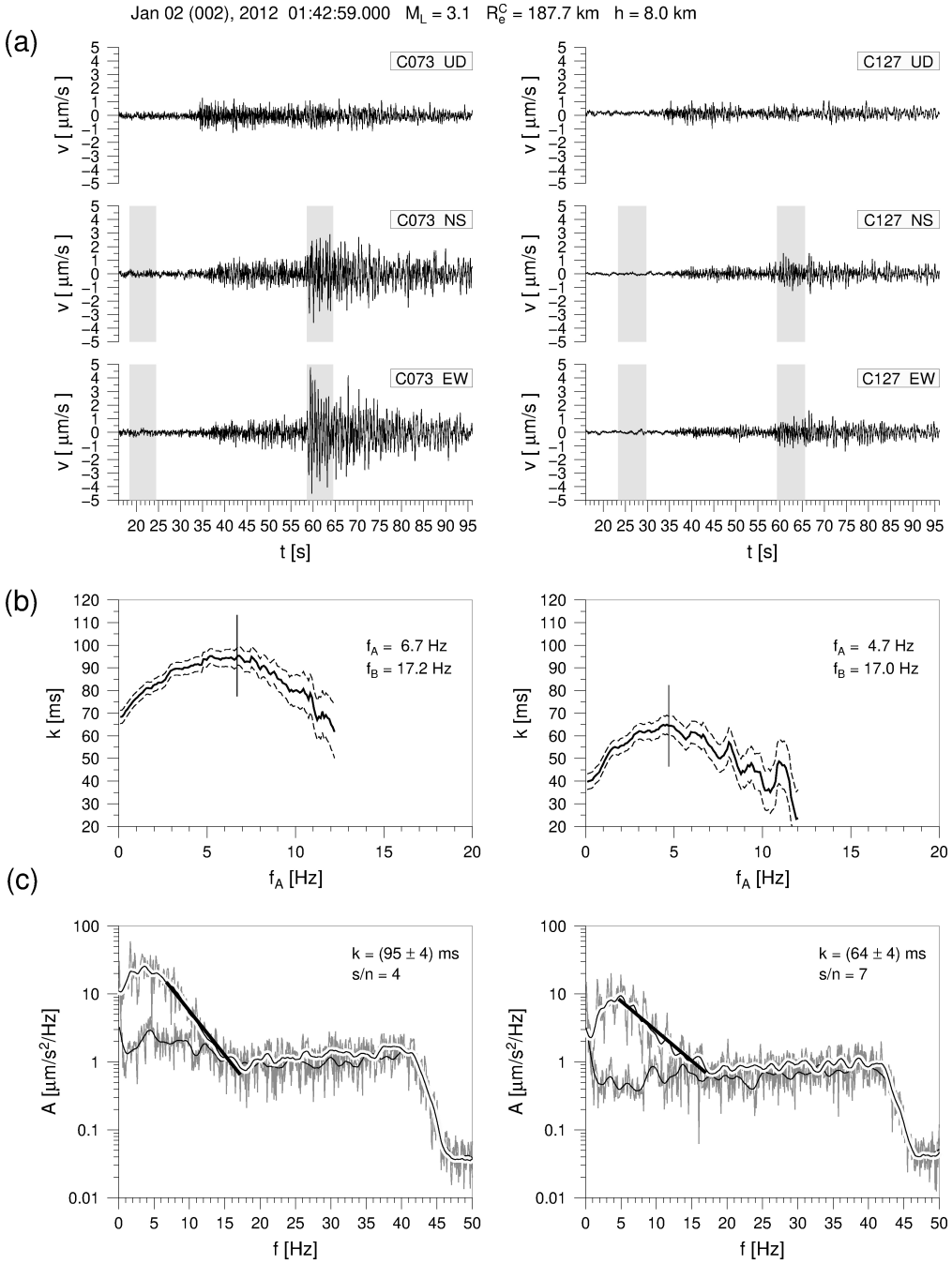

Figure S5. Example of k-record estimation: 2 January 2012 M_L=3.1 event, recorded by stations C073 (surface) and C127 (borehole). R_e^C is the epicentral distance measured from the center of the network. h is depth. (a): velocity records (vertical, NS and EW components) and time windows employed for noise and signal analysis (grey areas). (b): k-record estimates and standard deviations as a function of the lower limit of the frequency band adopted for the linear regression, f_A (solid and dashed lines, respectively). The adopted values of f_A and f_B are also indicated, and the vertical segment marks the chosen value of f_A. (c): signal and noise maximized acceleration spectra and linear regressions used to obtain the k-record estimate. Grey lines: original spectra of signal and noise; black thin line: smoothed noise spectrum; highlighted black thin line: smoothed signal spectrum; black thick line: linear regression. Signal-to-noise ratios, s/n, and k-record estimates are also indicated.

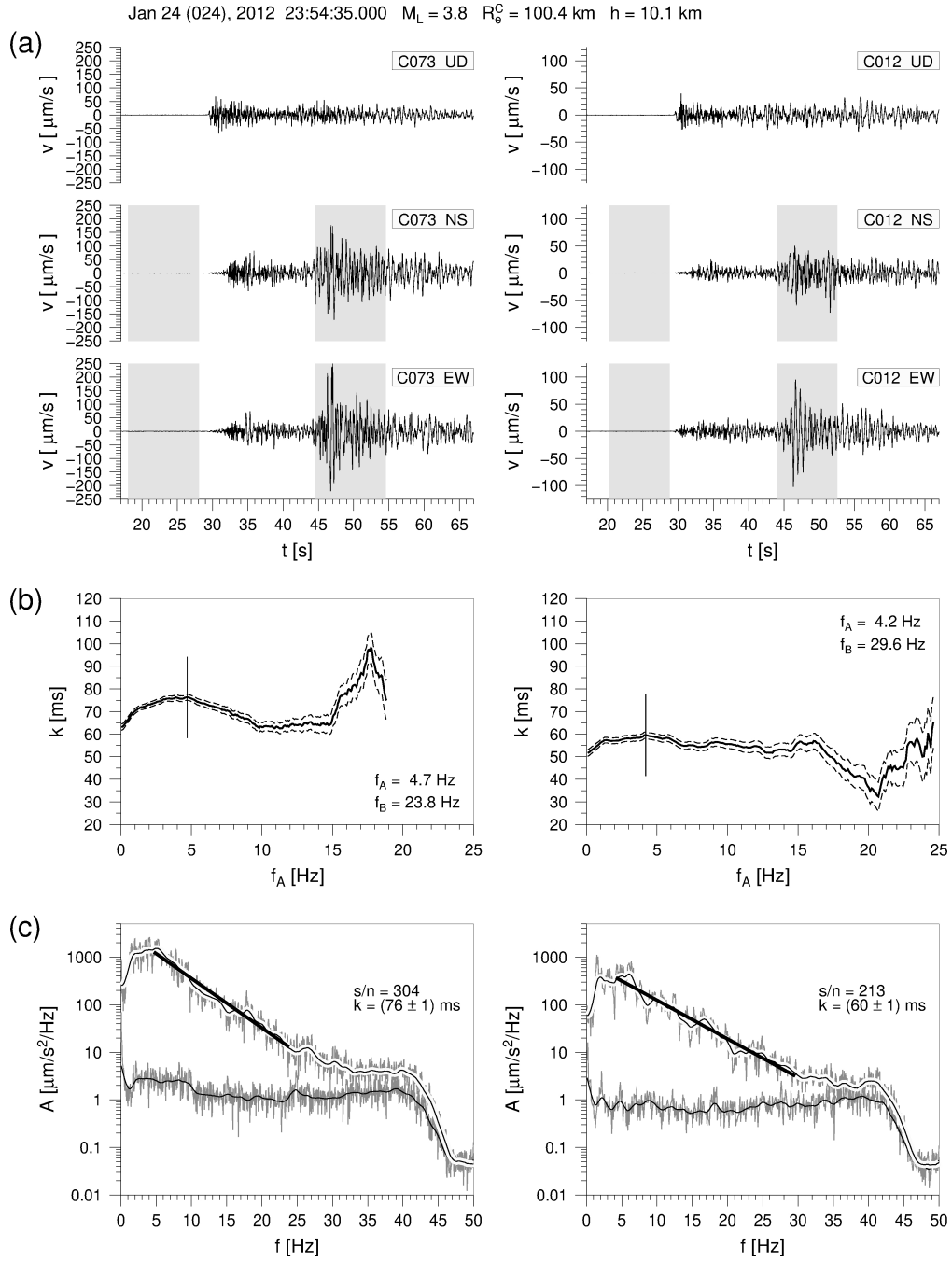

Figure S6. Example of k-record estimation: 24 January 2012 M_L=3.8 event, recorded by stations C073 (surface) and C012 (borehole). R_e^C is the epicentral distance measured from the center of the network. h is depth. (a): velocity records (vertical, NS and EW components) and time windows employed for noise and signal analysis (grey areas). (b): k-record estimates and standard deviations as a function of the lower limit of the frequency band adopted for the linear regression, f_A (solid and dashed lines, respectively). The adopted values of f_A and f_B are also indicated, and the vertical segment marks the chosen value of f_A. (c): signal and noise maximized acceleration spectra and linear regressions used to obtain the k-record estimate. Grey lines: original spectra of signal and noise; black thin line: smoothed noise spectrum; highlighted black thin line: smoothed signal spectrum; black thick line: linear regression. Signal-to-noise ratios, s/n, and k-record estimates are also indicated.

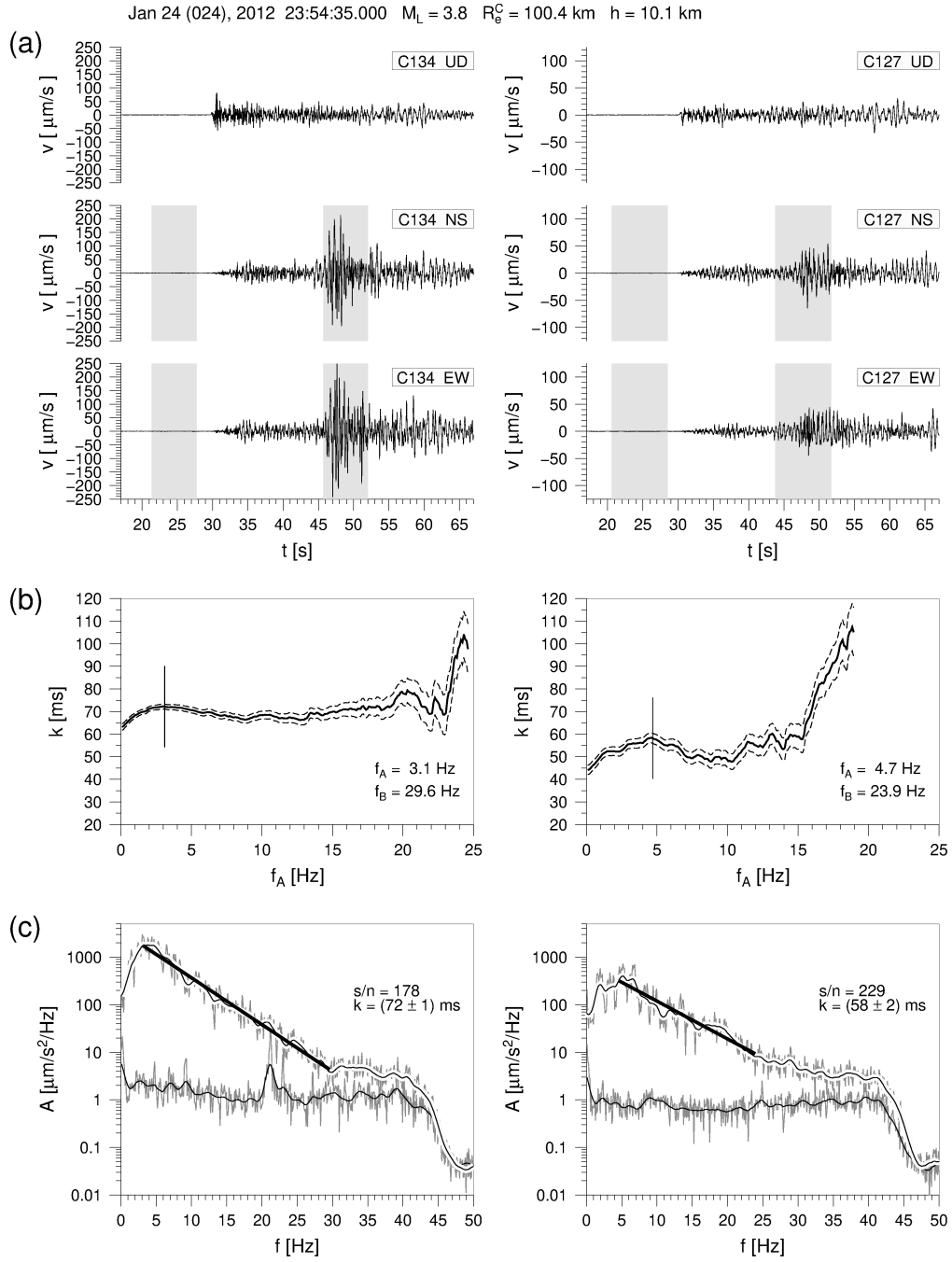

Figure S7. Example of k-record estimation: 24 January 2012 M_L=3.8 event, recorded by stations C134 (surface) and C127 (borehole). R_e^C is the epicentral distance measured from the center of the network. h is depth. (a): velocity records (vertical, NS and EW components) and time windows employed for noise and signal analysis (grey areas). (b): k-record estimates and standard deviations as a function of the lower limit of the frequency band adopted for the linear regression, f_A (solid and dashed lines, respectively). The adopted values of f_A and f_B are also indicated, and the vertical segment marks the chosen value of f_A. (c): signal and noise maximized acceleration spectra and linear regressions used to obtain the k-record estimate. Grey lines: original spectra of signal and noise; black thin line: smoothed noise spectrum; highlighted black thin line: smoothed signal spectrum; black thick line: linear regression. Signal-to-noise ratios, s/n, and k-record estimates are also indicated.

2 METHODS TO CALCULATE $\Delta k^J_{0_{100}}$, k^J_0 AND m

In order to reduce the high variability usually affecting the measurements of k-record we have implemented four different methods to calculate $\Delta k^J_{0_{100}}$, k^J_0 and m. All methods rely on the choice of a reference borehole station, such that, named as k^{REF}_0 the site-specific kappa of the reference, we can express the site-specific kappa of station J as:

$$k^J_0 = \Delta k^J_{0_{100}} + k^{REF}_0 \tag{S1}$$

(see eq. (11) in the text). The following procedures are applied in order to compute the above parameters from the obtained k-record values,

(A) For each station J, we assume a linear dependence of k on epicentral distance according to:

$$k^{I,J}(R_e{}^{I,J}) = k^J_0 + m^J \cdot R_e{}^{I,J} \tag{S2}$$

Using data from selection 1 we solve the M equations given by (S2) for the $2M$ unknowns: k^J_0 and m^J, M being the number of stations. $k^{I,J}$, which depends on epicentral distance $R_e{}^{I,J}$, is the estimated k-record value obtained with velocity data of earthquake I, recorded at station J. Solutions are searched through the weighted least-square method with weights assigned to the k-record data as: $w^{I,J} = (\delta_0/\delta k^{I,J})^2$, where $\delta k^{I,J}$ is the uncertainty of the slope of the high frequency MS and $\delta_0 = 1$ ms. The depth limit of 25 km, characterizing the data of selection 1, assures compatibility with the hypothesis of incremental attenuation due to predominantly horizontal propagation through the crust, followed by an almost vertical propagation through geological structures beneath the site. Afterwards, we choose a reference borehole station according to eq. (S1) and apply the corresponding relations to compute each $\Delta k^J_{0_{100}}$ and the standard error, $\sigma_{\Delta k^J_{0_{100}}}$, through error propagation.

(B) Since epicentral distances are much greater than inter-station distances, the distance dependence of k is expected to be the same for all stations. Therefore, we replace eq. (S2) with the following, where m represents the common linear trend with distance:

$$k^{I,J}(R_e{}^{I,J}) = k^J_0 + m \cdot R_e{}^{I,J} \tag{S3}$$

Using data from selection 1 we solve eq. (S3) for k^J_0 and m. Then, we choose the same reference

station defined in (A) and apply eq. (S1) to compute $\Delta k^J_{0_{100}}$. Standard errors: $\sigma_{k^J_0}$; σ_m and $\sigma_{\Delta k^J_{0_{100}}}$, are computed as in (A).

(C) In order to minimize the bias due to source effect (f_c) and crustal attenuation on Δk_0, we separate the estimates of the quantities $\Delta k^J_{0_{100}}$ from that of m by grouping eqs. (S3) and (S1) as follows:

$$k^{I,J}(R_e^{I,J}) - \Delta k^J_{0_{100}} = k_0^{REF} + m \cdot R_e^{I,J} \tag{S4}$$

To solve eq. (S4) for k_0^{REF} and m, we need to estimate each $\Delta k^J_{0_{100}}$ in advance. For this purpose we consider the data of selection 2 and, for each station J except for the reference, we use the k-record values, $k^{I,J}$, to compute the quantities:

$$\Delta k^{I,J}_{0_{100}} = k^{I,J} - k^{I,REF} \tag{S5}$$

where the index I refers to earthquakes. For each J, I takes values from 1 to $N_{J,REF}$, $N_{J,REF}$ being the number of events recorded simultaneously by station J and the reference station. Each $\Delta k^J_{0_{100}}$ is then computed as weighted mean on index I of $\Delta k^{I,J}_{0_{100}}$. Weights are defined as: $w^{I,J} = 1/\sigma^2_{\Delta k^{I,J}_{0_{100}}}$, $\sigma_{\Delta k^{I,J}_{0_{100}}}$ being the error of $\Delta k^{I,J}_{0_{100}}$. It is worth noting that, compared to selection 1, the data selected for this task are characterized by a greater number of events. Indeed, aiming to calculate Δk_0, for this type of analysis we remove the constraint on depth which is necessary when the epicentral distance dependence is investigated. The data of selection 2 are moreover characterized by higher M_L. As second step, using data of selection 1, we solve eq. (S4) for k_0^{REF} and m, and then, for each station except for the reference, we compute k_0^J through eq. (S1). Solutions are searched through the weighted least-square method with weights defined as in (A). Standard errors $\sigma_{k^J_0}$ are computed through error propagation.

(D) Method (C) requires coincident recordings between each station and the reference which generally implies a reduction of available events. To overcome this limitation we thus consider the following further method for the computation of $\Delta k^J_{0_{100}}$, k_0^J and m. Since epicentral distances are much greater than inter-station distances, for each earthquake I we define the average event kappa, $\overline{k}^I$, characterized by a linear dependence on epicentral distance measured from the center of the network, R_e^C, given by:

$$\overline{k}^I(R_e^C) = k_0^C + m \cdot R_e^C \tag{S6}$$

For each earthquake I, the k-record measured at station J, $k^{I,J}$, is given by the contribution

of $\overline{k}^I$ and r_k^J, the station residual. The latter is independent on event and the sum of residuals is set to 0. Therefore, the following relationships apply:

$$k^{I,J} = \overline{k}^I + r_k^J \tag{S7}$$

$$\sum_{J=1}^{M} r_k^J = 0 \tag{S8}$$

Using data from selection 2 we solve the linear system consisting of eqs. (S7) and (S8) for $\overline{k}^I$ and r_k^J, through a weighted least square method with weights defined as in (A). As second step, we employ the data of selection 1 to solve eq. (S6) for k_0^C and m. We apply a weighted least square linear regression with weights given by: $w^I = \left(\sigma_0/\sigma_{\overline{k}^I}\right)^2$, $\sigma_{\overline{k}^I}$ being the standard error of $\overline{k}^I$ and $\sigma_0 = 1$ ms. Finally, for each station J, the site-specific kappa is computed by:

$$k_0^J = k_0^C + r_k^J \tag{S9}$$

and, using station residuals, the corresponding $\Delta k_{0_{100}}$ is calculated as:

$$\Delta k_{0_{100}}^J = r_k^J - r_k^{REF} \tag{S10}$$

Standard errors $\sigma_{k_0^J}$ and $\sigma_{\Delta k_{0_{100}}^J}$ are computed through error propagation.

3 EXAMPLES OF INTERFERENCE FREQUENCIES ESTIMATION

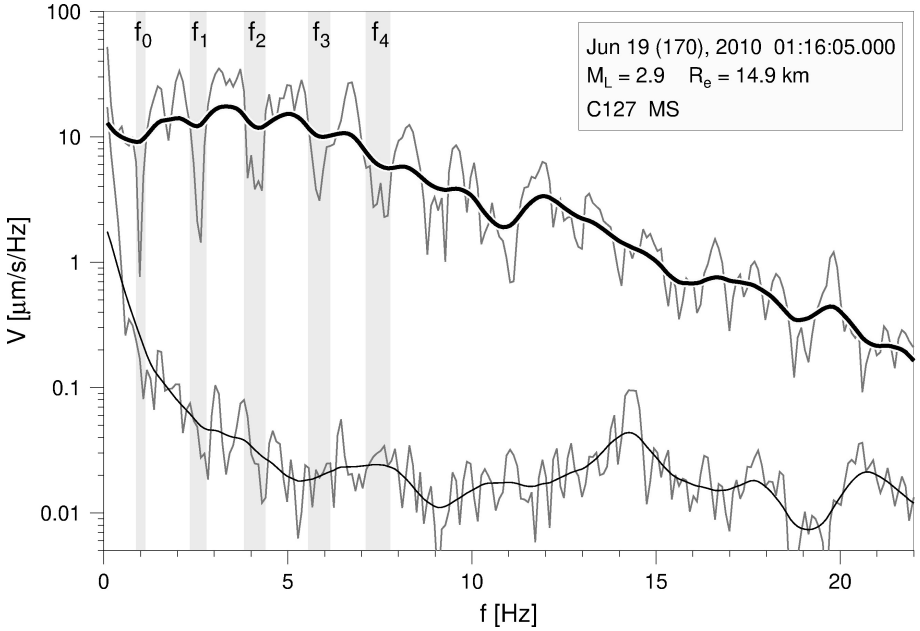

Figure S8. Example of interference frequencies estimation. 19 June 2010 M_L=2.9 event, recorded at 14.9 km epicentral distance by station C127. Grey lines: original maximized velocity spectra of signal and noise; black thick and thin lines: smoothed maximized velocity spectrum of signal and noise, respectively; grey areas: measurement errors of the interference frequencies: $f_N,\ N = 0, 4$.

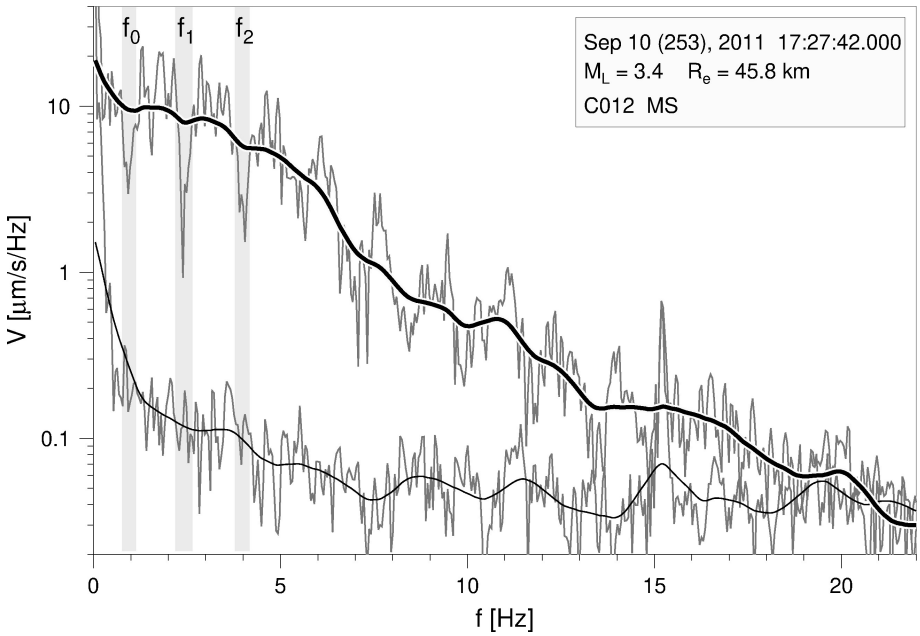

Figure S9. Example of interference frequencies estimation. 10 September 2011 M_L=3.4 event, recorded at 45.8 km epicentral distance by station C012. Grey lines: original maximized velocity spectra of signal and noise; black thick and thin lines: smoothed maximized velocity spectrum of signal and noise, respectively; grey areas: measurement errors of the interference frequencies: $f_N,\ N = 0, 2$.

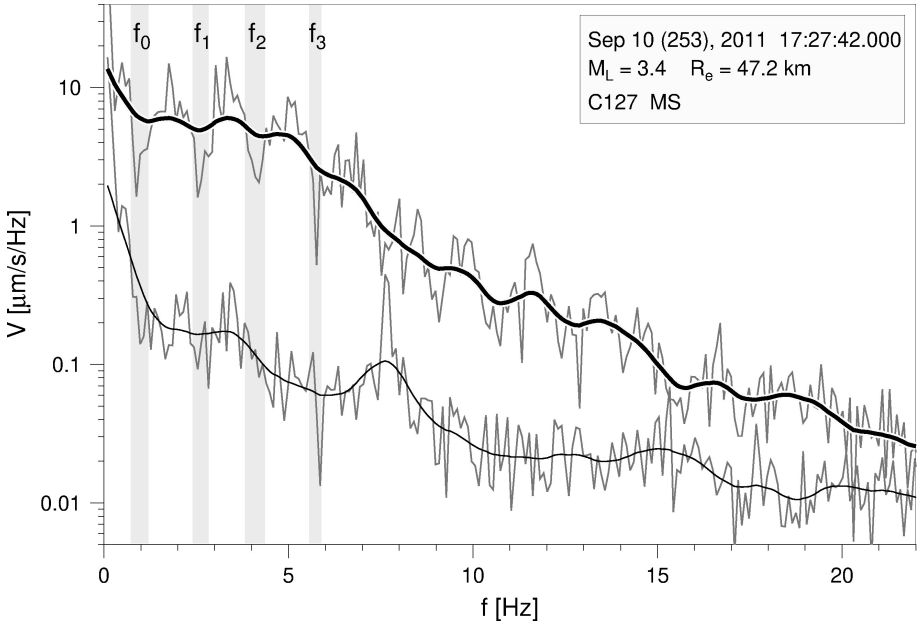

Figure S10. Example of interference frequencies estimation. 10 September 2011 M_L=3.4 event, recorded at 47.2 km epicentral distance by station C127. Grey lines: original maximized velocity spectra of signal and noise; black thick and thin lines: smoothed maximized velocity spectrum of signal and noise, respectively; grey areas: measurement errors of the interference frequencies: $f_N,\ N = 0, 3$.

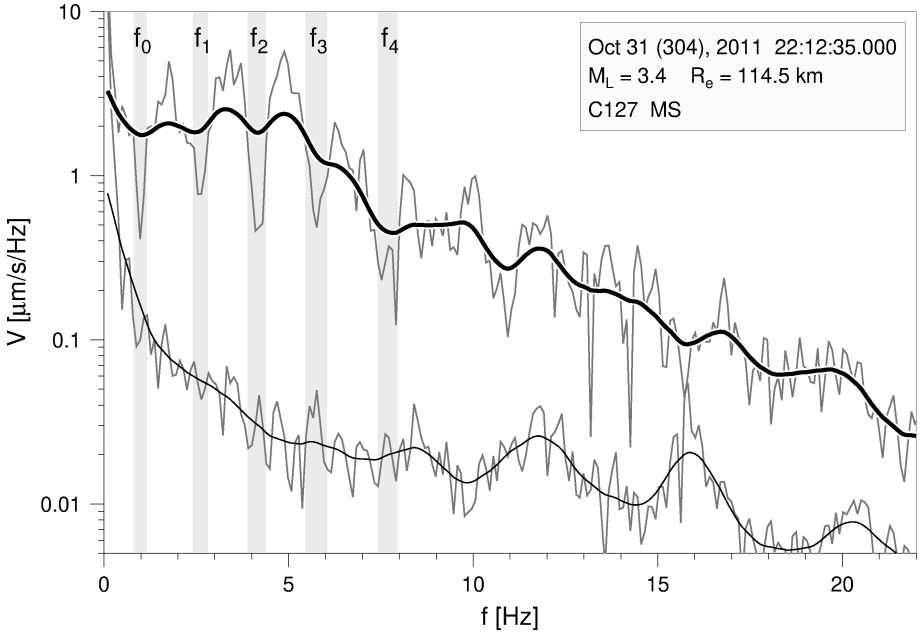

Figure S11. Example of interference frequencies estimation. 31 October 2011 M_L=3.4 event, recorded at 114.5 km epicentral distance by station C127. Grey lines: original maximized velocity spectra of signal and noise; black thick and thin lines: smoothed maximized velocity spectrum of signal and noise, respectively; grey areas: measurement errors of the interference frequencies: $f_N,\ N = 0, 4$.

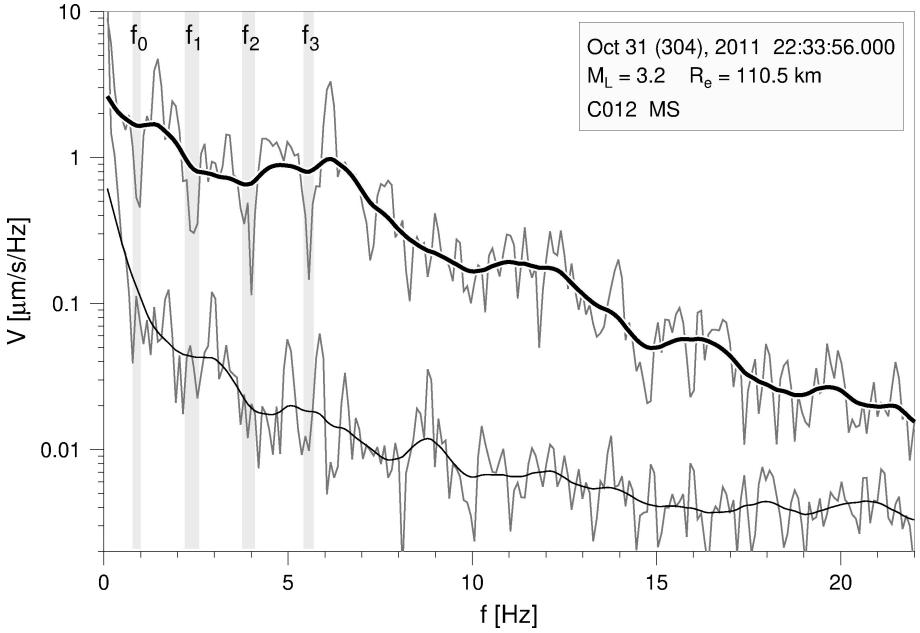

Figure S12. Example of interference frequencies estimation. 31 October 2011 M_L=3.2 event, recorded at 110.5 km epicentral distance by station C012. Grey lines: original maximized velocity spectra of signal and noise; black thick and thin lines: smoothed maximized velocity spectrum of signal and noise, respectively; grey areas: measurement errors of the interference frequencies: $f_N,\ N = 0, 3$.

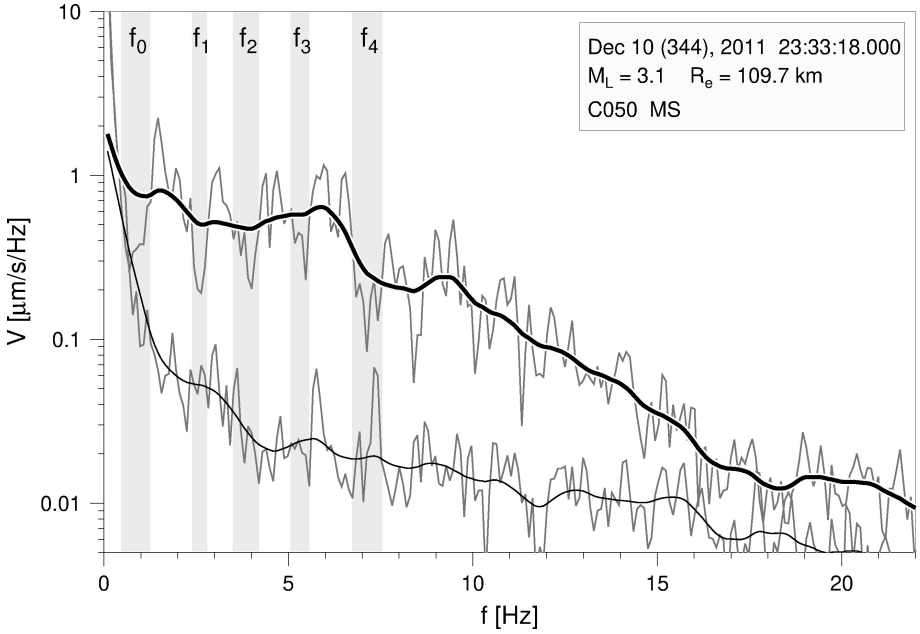

Figure S13. Example of interference frequencies estimation. 10 December 2011 M_L=3.1 event, recorded at 109.7 km epicentral distance by station C050. Grey lines: original maximized velocity spectra of signal and noise; black thick and thin lines: smoothed maximized velocity spectrum of signal and noise, respectively; grey areas: measurement errors of the interference frequencies: $f_N,\ N = 0, 4$.

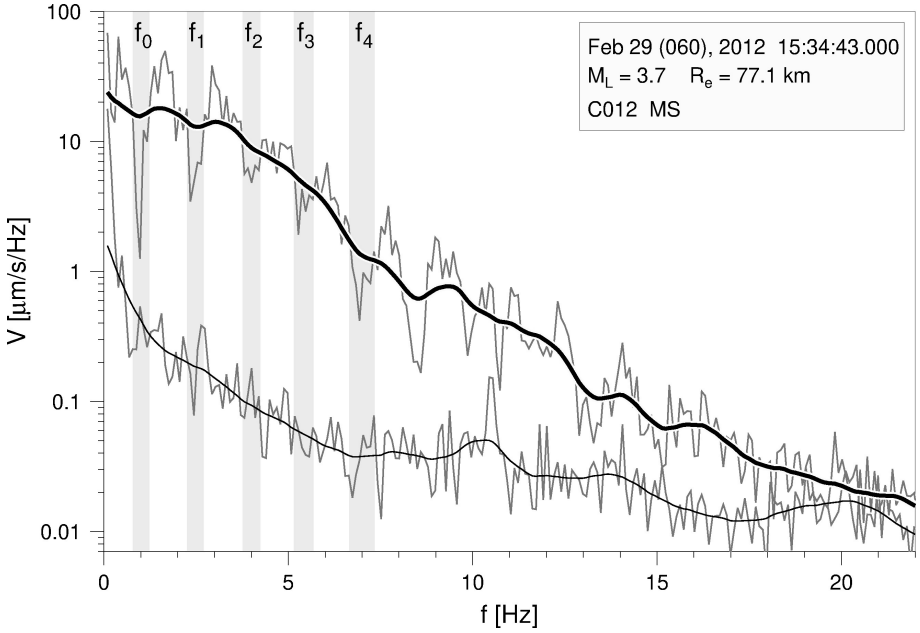

Figure S14. Example of interference frequencies estimation. 29 February 2012 M_L=3.7 event, recorded at 77.1 km epicentral distance by station C012. Grey lines: original maximized velocity spectra of signal and noise; black thick and thin lines: smoothed maximized velocity spectrum of signal and noise, respectively; grey areas: measurement errors of the interference frequencies: $f_N,\ N = 0, 4$.

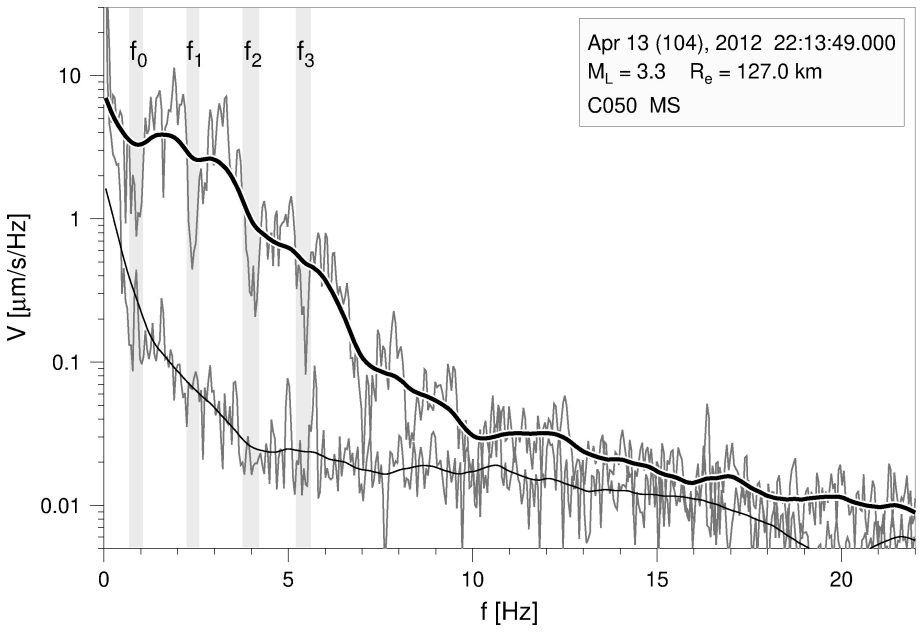

Figure S15. Example of interference frequencies estimation. 13 April 2012 M_L=3.3 event, recorded at 127.0 km epicentral distance by station C050. Grey lines: original maximized velocity spectra of signal and noise; black thick and thin lines: smoothed maximized velocity spectrum of signal and noise, respectively; grey areas: measurement errors of the interference frequencies: $f_N,\ N = 0, 3$.

4 DIFFERENCE BETWEEN ADJACENT INTERFERENCE FREQUENCIES

4.1 Method to calculate Δf^J

Assuming a vertical propagation, for each selected earthquake I, recorded at the borehole station J, we measure the frequencies $f_N^{I,J}$ where seismic wave interference produces spectral "holes" on the corresponding MS. Each $f_N^{I,J}$ is measured by picking the frequencies $f_{Na}^{I,J}$ and $f_{Nb}^{I,J}$, taking the mean value as: $f_N^{I,J} = (f_{Na}^{I,J} + f_{Nb}^{I,J})/2$ and estimating the measurement error as: $\delta f_N^{I,J} = (f_{Nb}^{I,J} - f_{Na}^{I,J})/2$. We consider up to 5 frequencies $f_N^{I,J}$ with: $N = 0, ...4$, superimposing for each record the original MS, the smoothed MS and the MS of noise, computed on an equal-length time window selected before the first P-wave arrival. Figs. S8, S9, S10, S11, S12, S13, S14 and S15 show some examples of $f_N^{I,J}$ estimation.

Afterwards, in order to measure the frequency difference between two adjacent interference frequencies observed at each station, Δf^J, we apply the following procedure:

(1) by considering all events, we compute each frequency f_N^J $(N = 0, ...4)$ and the corresponding uncertainty as weighted mean on index I of the interference frequencies $f_N^{I,J}$.
We define weights as: $w^{I,J} = 1/\delta^2 f_N^{I,J}$ and, in order to avoid incompatibility with the spectral resolution of velocity data, we also impose: $\delta f_N^{I,J} > 0.12$ Hz.

(2) f_N^J values are employed to calculate: $\Delta f_{N,N+1}^J = f_{N+1}^J - f_N^J$ $(N = 0, ...3)$;

(3) Δf^J and the corresponding standard error, $\sigma_{\Delta f^J}$, is computed as weighted mean on index N of: $\Delta f_{N,N+1}^J$ $(N = 0, ...3)$.

4.2 Results

Fig. S16 shows the difference between adjacent interference frequencies,$\Delta f^J_{N,N+1}$, computed for each station of the network with $N = 0, ...3$, and the corresponding mean $\pm$ 1 standard errors, Δf^J (see also Section 5.2 - Table 4.).

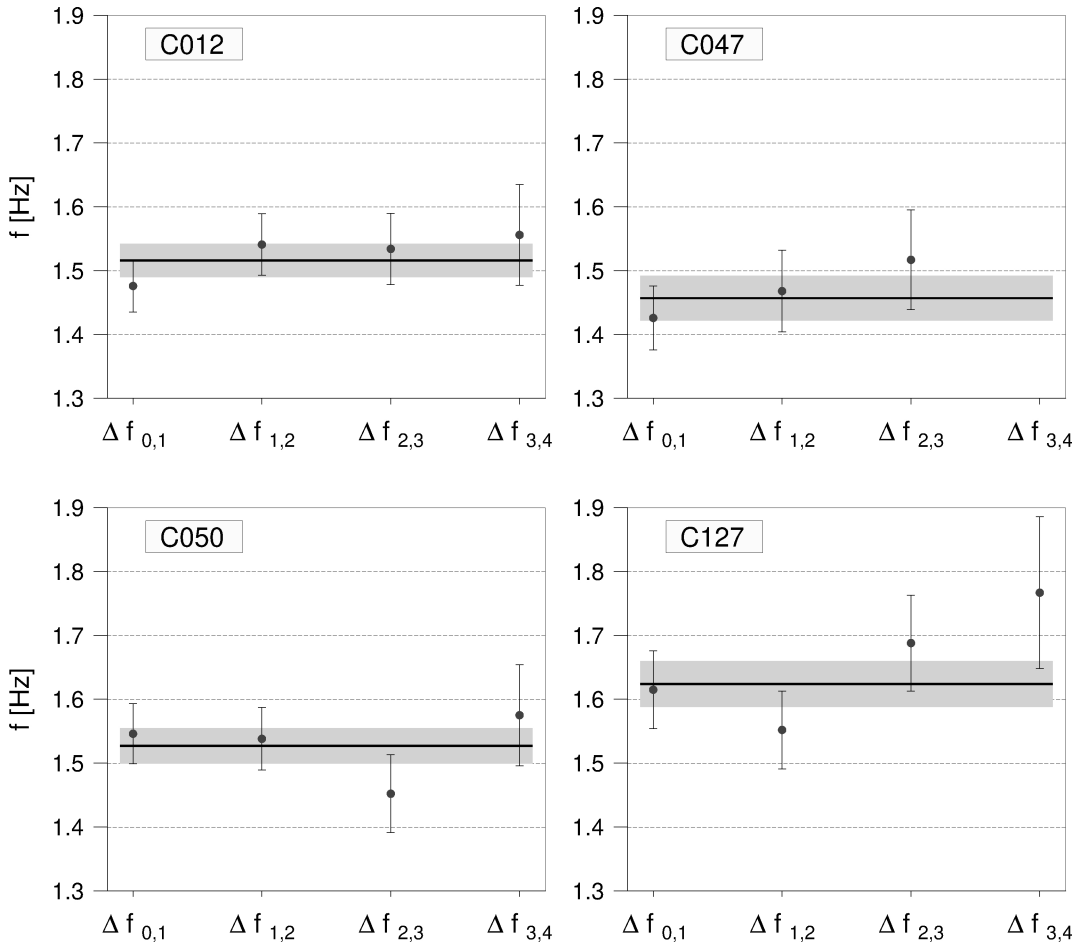

Figure S16. Differences between adjacent interference frequencies estimated with the borehole stations of the microseismic network. Closed circles with error bars represent the differences $\Delta f_{N,N+1}$ (N = 0, 3), estimated with the interference frequencies f_N ($N = 0, 4$). Solid lines and grey areas represent the mean and $\pm$1 standard errors, respectively.